

Structure-Consistent Weakly Supervised Salient Object Detection with Local Saliency Coherence

Siyue Yu¹, Bingfeng Zhang¹, Jimin Xiao^{1*}, Eng Gee Lim¹

¹School of Advanced Technology, Xi'an Jiaotong Liverpool University

siyue.yu@xjtlu.edu.cn, bingfeng.zhang@xjtlu.edu.cn, jimin.xiao@xjtlu.edu.cn, enggee.lim@xjtlu.edu.cn

Abstract

Sparse labels have been attracting much attention in recent years. However, the performance gap between weakly supervised and fully supervised salient object detection methods is huge, and most previous weakly supervised works adopt complex training methods with many bells and whistles. In this work, we propose a one-round end-to-end training approach for weakly supervised salient object detection via scribble annotations without pre/post-processing operations or extra supervision data. Since scribble labels fail to offer detailed salient regions, we propose a local coherence loss to propagate the labels to unlabeled regions based on image features and pixel distance, so as to predict integral salient regions with complete object structures. We design a saliency structure consistency loss as self-consistent mechanism to ensure consistent saliency maps are predicted with different scales of the same image as input, which could be viewed as a regularization technique to enhance the model generalization ability. Additionally, we design an aggregation module (AGGM) to better integrate high-level features, low-level features and global context information for the decoder to aggregate various information. Extensive experiments show that our method achieves a new state-of-the-art performance on six benchmarks (e.g. for the ECSSD dataset: $F_\beta = 0.8995$, $E_\xi = 0.9079$ and $MAE = 0.0489$), with an average gain of 4.60% for F-measure, 2.05% for E-measure and 1.88% for MAE over the previous best method on this task. Source code is available at <http://github.com/siyueyu/SCWSSOD>.

Introduction

Salient object detection (SOD) aims to detect the most attractive regions in an image according to the human perception. It can be further applied in different computer vision tasks, such as image-sentence matching (Ji et al. 2019), image segmentation (Sun and Li 2019) and image retrieval (Wang et al. 2020a). In the last decade, deep learning based salient object detection algorithms (Chen et al. 2020; Liu et al. 2019; Qin et al. 2019) have become popular due to their superior performance. These methods usually design different modules to help their networks learn better feature representations for saliency prediction. However, they are

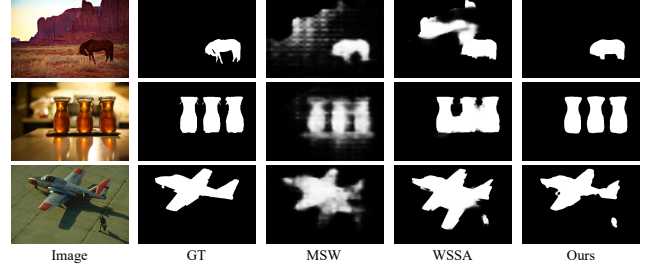


Figure 1: Our predicted saliency maps are compared with that of other weakly supervised methods. From left to right: Input image; Ground-truth; MSW (Zeng et al. 2019); WSSA (Zhang et al. 2020b); Ours.

highly dependent on pixel-wise saliency labels, which are time-consuming and costly with manual annotations.

In recent years, sparse labeling methods have attracted much attention. Many weakly supervised salient object detection methods have been proposed to improve label efficiency while maintaining model performance. Image level labels are utilized in some methods (Wang et al. 2017; Li, Xie, and Lin 2018) to learn salient object detection. However, these works usually use image-level tags for saliency localization and then further train their models with predicted saliency maps through multiple-stage learning. Besides, some other works (Nguyen et al. 2019; Zhang, Han, and Zhang 2017) train their models with noisy pseudo labels from handcrafted methods and/or predicted maps by other weakly supervised SOD models, where pre-processing steps are used to clean noisy labels. All above mentioned works need complex training steps to obtain final saliency maps.

Additionally, scribble annotations are proposed recently due to their flexibility to label winding objects and low-cost compared to annotating per-pixel saliency masks. However, scribble annotations cannot cover the whole object region or directly provide object structure. Therefore, edge detection is used in the framework (Zhang et al. 2020b) to obtain object boundaries, and the SOD model is trained with predicted edge maps from other trained edge detection models. However, this step introduces extra data information into the SOD training process to recover integral object structure. The training process of (Zhang et al. 2020b) is also complex,

*Corresponding Author.

Copyright © 2021, Association for the Advancement of Artificial Intelligence (www.aaai.org). All rights reserved.

as they design a scribble boosting scheme to iteratively train their model using initial saliency predictions to obtain higher quality saliency maps.

In this paper, we aim to tackle the aforementioned issues in existing weakly supervised SOD methods. Specifically, we aim to design a high performance SOD method with scribble annotations via one-stage end-to-end training, where no pre/post-processing steps nor extra supervision (e.g., edge maps) will be used. To mitigate the issue of poor boundary localization caused by scribble annotations and partial cross-entropy loss (Zhang et al. 2020b), we design a local saliency coherence loss to provide supervision for unlabeled points, based on the idea that points with similar features and/or close positions should have similar saliency values. By doing this, we take advantage of intrinsic properties of an image instead of extra edge or other assisting information to help our model learn better object structure and predict integral salient regions.

Besides, we find that weakly supervised SOD models fail to predict consistent saliency maps with different scales of the same image as input. To handle this problem, we propose a saliency structure consistency loss, which could be viewed as a regularization technique to enhance the model generalization ability.

Additionally, global context information can infer the relationship of different salient regions and help network predict better results (Chen et al. 2020). High-level features can provide better semantic information and low-level features can capture rich spatial information (Hou et al. 2017). In the decoder layers, we design an aggregation module called AGGM to integrate all information for better feature representations using the attention mechanism (Shi et al. 2020).

With our specially designed loss functions and network structures, our model can predict saliency maps close to human perception. Some obtained saliency maps are illustrated in Fig. 1. Our method predicts smoother and integral saliency objects even for the challenging cases with background disturbance, object shadow, and multiple objects. In general, our main contributions can be summarized as:

- A local saliency coherence loss is proposed for scribble supervised saliency object detection, which helps our network to learn integral salient object structures without any extra assisting data or complex training process.
- A self-consistent mechanism is introduced to ensure that consistent saliency masks will be predicted with different scales of the same image as input. It is an effective regularization to enhance the model generalization ability.
- An aggregation module named AGGM is designed in the encoder-decoder framework for weakly supervised SOD, which effectively aggregates global context information as well as high-level and low-level features.
- Comprehensive experiments show that our approach achieves a new state-of-the-art performance compared with other scribble supervised SOD algorithms on six widely-used benchmarks, with an average gain of 4.60% for F-measure, 2.05% for E-measure and 1.88% for MAE over the previous best performing method.

Related Work

Salient Object Detection. CNN based salient object detection is popular due to its superior performance under the fully supervised setting. Most proposed methods (Chen et al. 2020; Zhang et al. 2018b; Pang et al. 2020) studied how to aggregate multi-level features in the network to better capture features for salient regions. Some works (Qin et al. 2019; Wang et al. 2019; Zhao et al. 2019) introduced edge supervision to learn object boundary and in turn refine their saliency predictions with better object structures. However, these methods need fully pixel-level annotations, which are costly and time-consuming. Thus, in this paper, we focus on weakly supervised salient object detection.

Weakly Supervised Salient Object Detection. With recent advances in weakly supervised learning, SOD considers weakly supervised or unsupervised learning to ease the burden on pixel level annotations. WSS (Wang et al. 2017) firstly proposed to learn SOD through image-level labels to reduce annotation efforts. They proposed a global smooth pooling layer and a foreground inference network to maintain prediction quality for unseen categories during inference. Additionally, MSW (Zeng et al. 2019) utilized diverse supervision sources including category labels, captions and noisy pseudo labels to train their network via their attention transfer loss. Besides, user-friendly scribble annotations was proposed in (Zhang et al. 2020b), which took only 1~2 seconds to label one image. To simplify training procedures and narrow the gap between weakly and fully supervised methods, we propose an end-to-end training approach containing one-round training without post-processing.

Weakly Supervised Semantic Segmentation. Various types of weak annotations were proposed to save human labor expense for semantic segmentation. Bounding boxes were used in BCM (Song et al. 2019) to provide the regions of foreground objects. Khoreva et al (Khoreva et al. 2017) explored bounding box supervisor for both instance and semantic segmentation. Berman et al (Bearman et al. 2016) proposed point-level supervision. DEXTR (Maninis et al. 2018) made the use of both bounding box and point seed label to predict semantic segmentation. Additionally, AE (Chen et al. 2018) presented a new interactive segmentation by balancing the selection and defocus cues at phototaking based on point-level supervision. RRM (Zhang et al. 2020a) proposed a fully end-to-end training method to learn to predict segmentation maps through image-level labels. Additionally, SEAM (Wang et al. 2020b) designed a self-supervised equivariant attention mechanism to supervise CAM with image-level labels. ScribbleSup (Lin et al. 2016) used a graphical model to learn from scribbles. Besides, Normalized cut loss (Tang et al. 2018a) and kernel cut loss (Tang et al. 2018b) were proposed to regularize cross entropy loss for semantic segmentation with scribble annotations. Although scribble annotations for semantic segmentation have been intensively studied, little effort was devoted on SOD with scribble labels.

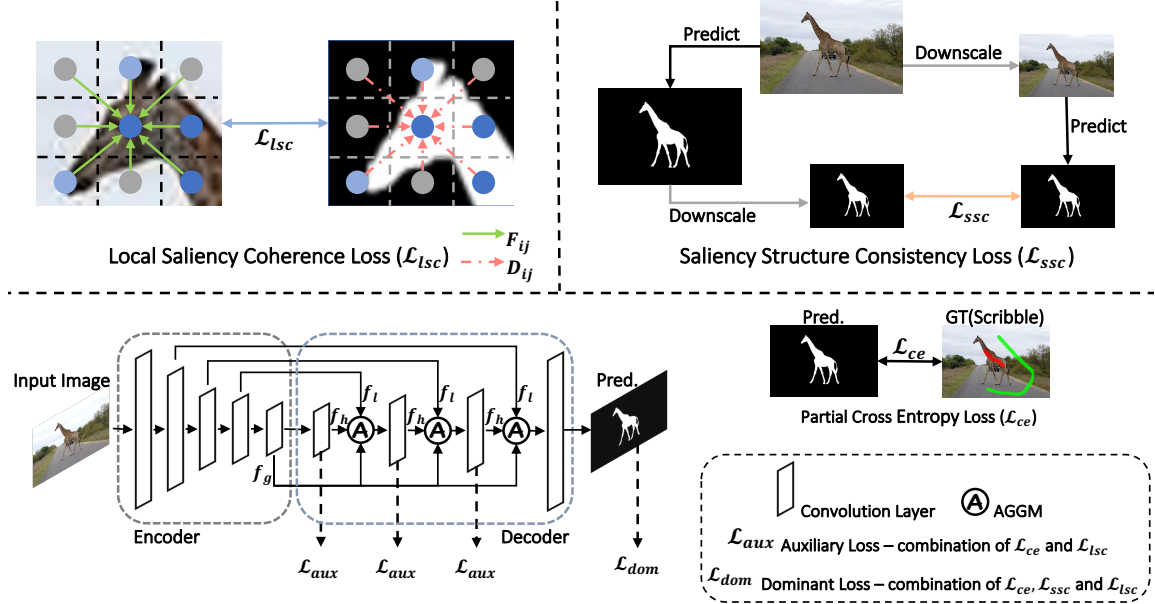


Figure 2: The framework of our network and learning procedure. Specifically, f_l , f_h , f_g denote to the low-level, high-level features and global context information, respectively. The AGGM is applied in the decoder to integrate multi-level features. The proposed local saliency coherence loss and saliency structure consistency loss are applied with partial cross entropy loss to optimize the network as a dominant loss. To facilitate optimization, our local saliency coherence loss are applied with partial cross entropy loss as auxiliary losses to further supervise intermediate low-resolution saliency maps.

Methodology

Overview

Firstly, the training dataset is defined as $U = \{x_n, y_n\}_{n=1}^N$, where x_n is the input image, y_n is the corresponding label, and N is the total number of training images. Note that, in our task, the label y_n is annotated as scribble.

The whole network and learning framework are shown in Fig. 2. The network contains an encoder and a decoder, and the designed aggregation module AGGM is applied in each layer of the decoder. In this way, the three kinds of information can be better propagated into next layers. Sigmoid function is applied on the output of the decoder to normalize the output saliency values to $[0, 1]$. Thus, our network receives the input image and outputs the corresponding saliency map directly. During training, the proposed local saliency coherence loss and saliency structure consistency loss are applied with the partial cross entropy loss as the dominant loss to supervise the final predicted saliency map. Meanwhile, to facilitate training, we enforce an auxiliary loss, which includes the local saliency coherence loss and the partial cross entropy loss on each sub-stage to supervise the intermediate low-resolution saliency maps. Note that the intermediate low-resolution saliency maps are upsampled to the corresponding scale of x_n to supervise the intermediate low-resolution saliency map. In the following sections, we will discuss the AGGM and each loss in details.

Aggregation Module

Our network follows an encoder-decoder framework. The encoder layers learn different features of the salient regions

and further propagate them to the decoder. Since some detailed features might be diluted, each decoding layer uses output of preceding layer, the features of corresponding encoding layer and the global context information, which is the final output of the encoder, as inputs to predict salient regions. However, we argue that each input should be allocated to different weights for each decoding layer. To learn the importance of each input feature by self-learning, our aggregation module is designed as in Fig. 3. 3×3 convolution layers and global average pooling layers are applied to learn the importance of each input feature. Once the weights are obtained, normalization is applied, which can be written as:

$$f_{out} = \frac{w_h f_h + w_g f_g + w_l f_l}{w_h + w_g + w_l}, \quad (1)$$

where w_h , w_g and w_l are obtained weights. f_h , f_g and f_l are input multi-level features. With Eq. (1), the network can aggregate multi-level features and with our AGGM, the importance of each feature can be learned by self-learning.

Local Saliency Coherence Loss

For scribble annotations, there are a great number of unlabeled pixels. With only the given scribble labels, it is hard to learn rich information of salient regions. In addition, there is no category information in the SOD task, making it more difficult to learn object structures. Therefore, the network needs other supervision to get better saliency maps with clear object boundaries. In this case, we design a local saliency coherence loss to help network predict smooth saliency maps with the scribble annotations. We consider

that for pixel i and pixel j of the same input image, if they are with similar features or close positions, they tend to have similar saliency scores. On the other hand, if two points do not share similar features or they are distant from each other, they are more likely to have different saliency scores. We first define the saliency difference between two different pixels i and j as follows:

$$D(i, j) = |S_i - S_j|, \quad (2)$$

where S_i and S_j are the predicted saliency scores of pixels i and j , respectively. We use $L1$ distance to directly compute the discrepancy of the saliency scores.

Instead of computing the similarities between any two pixels in an image, which introduces too much background noise and takes too much GPU memory, we compute the discrepancy of a reference point with its adjacent points in a $k \times k$ kernel size. However, if we directly compute the loss using Eq. (2), the network fails to distinguish the salient region with background, especially for the pixels close to the boundaries. For pixels around object boundaries, their saliency scores are not always similar with their adjacent pixels. Therefore, we set a similarity energy between two pixels i and j , which is defined based on Gaussian kernel bandwidth filter (Obukhov et al. 2019), to draw close saliency scores for pixels with similar features and/or with small distance. Then, the final local saliency coherence loss is designed as:

$$\mathcal{L}_{lsc} = \sum_i \sum_{j \in K_i} F(i, j) D(i, j), \quad (3)$$

where K_i is the region covered by a $k \times k$ kernel around pixel i , and $F(i, j)$ denotes to the following filter:

$$F(i, j) = \frac{1}{w} \exp\left(-\frac{\|P(i) - P(j)\|^2}{2\sigma_P^2} - \frac{\|I(i) - I(j)\|^2}{2\sigma_I^2}\right), \quad (4)$$

where $1/w$ is the normalized weight, $P(\cdot)$ and $I(\cdot)$ are the position and RGB color of a pixel, respectively. σ_P and σ_I are hyper parameters for the scale of Gaussian kernels. $\|\cdot\|^2$ is an $L2$ operation.

The local saliency coherence loss \mathcal{L}_{lsc} enforces similar pixels in the kernel to share consistent saliency scores, which further propagates labeled points to the whole image during training. With the partial cross entropy loss to supervise labeled points, the network can acquire enlarged salient regions with limited labels without any extra information.

Self-consistent Mechanism

For a good salient object detection model, saliency maps predicted with different scales of the same image should be consistent. We define a salient object detection function as $f_\theta(\cdot)$ with parameter θ , and a transformation as $T(\cdot)$. Then, for an ideal $f_\theta(x)$, it should satisfy this equation:

$$f_\theta(T(x)) = T(f_\theta(x)). \quad (5)$$

However, we find that it is difficult for weakly supervised SOD networks to predict consistent saliency maps with different input scales, as shown in Fig. 4(a). Therefore, by considering Eq. (5) as a regularization, we design a structure

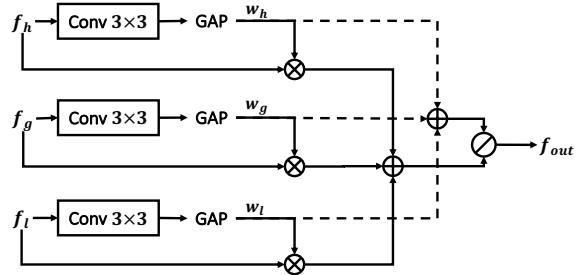


Figure 3: Framework of AGGM, where ‘GAP’ denotes to global average pooling, ‘ \times ’ is multiplication, ‘ $+$ ’ is addition and ‘ $/$ ’ is division.

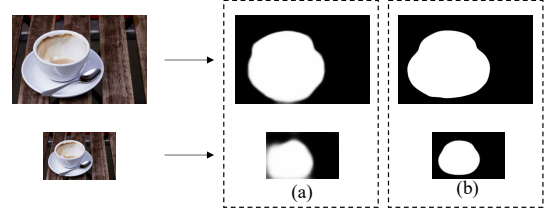


Figure 4: Comparison of predicted saliency maps for an input image with different scales: (a) without self-consistent mechanism; (b) with self-consistent mechanism.

consistency loss on predicted saliency maps from different input scales, which is defined as follows:

$$\mathcal{L}_{ssc} = \frac{1}{M} \sum_{u,v} \alpha \frac{1 - SSIM(S_{u,v}^\downarrow, S_{u,v}^\uparrow)}{2} + (1-\alpha) |S_{u,v}^\downarrow - S_{u,v}^\uparrow|, \quad (6)$$

where S^\downarrow is down-scaled predicted saliency map of a normal input image, S^\uparrow is the predicted saliency map of the same image with down-scaled size, and M is the number of pixels. SSIM denotes to the single scale SSIM (Wang et al. 2004; Godard, Mac Aodha, and Brostow 2017) and $\alpha = 0.85$ (Godard, Mac Aodha, and Brostow 2017). With Eq. (6), the network can learn more information on object structure and enhance generalization ability for different input scales. As shown in Fig. 4(b), with our self-consistent mechanism, the network can adapt to different scales and predict saliency maps with better object structure.

Objective Function

As shown in Fig. 2, our final loss function is the combination of a dominant loss and auxiliary losses following GCPANet (Chen et al. 2020). Specifically, a 3×3 convolution layer is conducted to squeeze the channel to 1 at each stage of the decoder to compute the saliency scores. Then, our proposed losses are used to cooperate with the partial cross entropy loss, which can be written as:

$$\mathcal{L}_{ce} = \sum_{i \in \tilde{\mathcal{Y}}} -y_i \log \hat{y}_i - (1 - y_i) \log(1 - \hat{y}_i), \quad (7)$$

where y denotes for ground-truth, \hat{y} is the predicted values and $\tilde{\mathcal{Y}}$ is the set of labeled pixels via scribble annotations.

The auxiliary loss \mathcal{L}_{aux} and dominant loss \mathcal{L}_{dom} can be written as:

$$\mathcal{L}_{aux}^q = \mathcal{L}_{ce} + \beta \mathcal{L}_{lsc} \quad q \in \{1, 2, 3\}, \quad (8)$$

$$\mathcal{L}_{dom} = \mathcal{L}_{ce} + \mathcal{L}_{ssc} + \beta \mathcal{L}_{lsc}, \quad (9)$$

where the hyper-parameter β shares the same value in Eq. (8) and Eq. (9), and q in Eq. (8) stands for the index of a decoder layer.

Finally, the overall objective function of our network is:

$$\mathcal{L}_{total} = \mathcal{L}_{dom} + \sum_{q=1}^3 \lambda_q \mathcal{L}_{aux}^q, \quad (10)$$

where λ_q is to balance the auxiliary loss of each stage, and we take the same value as in GCPANet (Chen et al. 2020).

Experiments

Implementation Details and Setup

Implementation Details. We use GCPANet (Chen et al. 2020) with backbone of ResNet-50 (He et al. 2016) pre-trained on ImageNet (Deng et al. 2009) as baseline. The partial cross entropy loss (Eq. (7)) is computed for background and foreground individually. w , σ_P , and σ_I in Eq. (4) are set to 1, 6 and 0.1, respectively. β in Eq. (8) and Eq. (9) is set to 0.3. The model is optimized by SGD with batch size of 16, momentum of 0.9 and weight decay of 5×10^{-4} . Additionally, we use triangular warm-up and decay strategies with the maximum learning rate of 0.01 and the minimum learning rate of 1×10^{-5} to train the network with 40 epochs. During training, each image is resized to 320×320 with random horizontal flipping and random cropping. In the inference stage, input images are simply resized to 320×320 and then fed into the network to predict saliency maps without any post-processing. All experiments are run on NVIDIA GeForce RTX 2080 Ti.

Datasets. We train our network on scribble annotated dataset S-DUTS (Zhang et al. 2020b) and evaluate our model on six widely-used salient object detection benchmarks: (1) ECSSD (Yan et al. 2013); (2) DUT-OMRON (Yang et al. 2013); (3) PASCAL-S (Li et al. 2014); (4) HKU-IS (Li and Yu 2015); (5) THUR (Cheng et al. 2014); (6) DUTS-TEST (Wang et al. 2017).

Baseline Methods and Evaluation Metrics. Our model is compared with 6 state-of-the-art weakly supervised or unsupervised SOD methods and 10 fully supervised SOD methods as baselines. We take three widely-used evaluation metrics for fair comparison: mean F-measure (F_β), mean E-measure (E_ξ) (Fan et al. 2018), and Mean Absolute Error (MAE) (Cong et al. 2017).

Comparison with State-of-the-arts

Quantitative Comparison. In Table 1, we compare our approach with other state-of-the-art approaches. It can be seen that our method achieves a new state-of-the-art performance among weakly supervised or unsupervised approaches under all the evaluation metrics. Our one-round

training method obtains an average gain of 4.60% for F_β , 2.05% for E_ξ , and 1.88% for MAE , compared with the previous best two-round training method WSSA (Zhang et al. 2020b) on the 6 datasets. Besides, our approach is comparable or even superior to some fully supervised methods, like PiCANet (Liu, Han, and Yang 2018), PAGR (Zhang et al. 2018b) and MLMSNet (Wu et al. 2019).

Qualitative Evaluation. We demonstrate some samples of our predicted saliency maps from the ECSSD dataset (Yan et al. 2013) in Fig. 5. It can be seen that our predicted saliency maps are more complete and precise compared with previous state-of-the-art weakly supervised methods (MSW and WSSA). Moreover, our approach is more general to different object classes and it is more robust to the disturbance of foreground-background (see rows 3 & 4 in Fig. 5). In some cases, our approach even performs better than fully supervised methods, such as CPD, BASNet and GCPANet (see rows 3 & 5 in Fig. 5).

Ablation Study

We conduct different ablation studies to analyze the proposed method, including the loss functions and our aggregation module. The experiments are evaluated on the DUTS-TEST dataset (Wang et al. 2017). We conduct the experiments by combining different parts of our method. As shown in Table 2, our method obtains the best performance using all the components, which illustrates that all the loss functions and the AGGM are necessary to realize the one-step training. We use GCPANet (Chen et al. 2020) as our baseline. If the network is directly trained with partial cross entropy loss, the results are relatively low, as listed in 1 of Table 2. This phenomenon shows that the partial cross entropy loss is insufficient for sparse labels. Moreover, comparing our final results with the baseline, we obtain gains of 11.61% for F_β , 4.73% for E_ξ and 1.54% for MAE , respectively.

Impact of AGGM. In Table 3, we evaluate the influence of our aggregation module AGGM when all the loss functions are enabled. It is interesting to see that using AGGM can obtain an average gain of 2.56% for F_β , 1.52% for E_ξ and 0.63% for MAE on DUT-OMRON and DUTS-TEST. However, when training without our proposed losses, as listed in 1 and 2 of Table 2, our AGGM contributes little compared with the baseline mode. This phenomenon shows that our AGGM is complementary with the proposed loss functions for sparse labels.

Impact of Saliency Structure Consistency Loss. We conduct this ablation study by adding saliency structure consistency loss to the baseline (AGGM is enabled). The results are shown in 3 of Table 2. Compared with only using partial cross entropy loss, using saliency structure consistency loss achieves the improvement of 5.29% for F_β , 2.81% for E_ξ and 0.47% for MAE . That is to say, our saliency structure consistency loss can regularize partial cross entropy loss and enhance the model generalization ability. Further, we evaluate the impact of SSIM in Eq. (6) which is shown in Table 4. We train the network using saliency structure consistency loss with and without SSIM separately. It can be seen that

Table 1: Comparison with other state-of-the-art approaches on 6 benchmarks. \uparrow means that larger is better and \downarrow denotes that smaller is better. The best performance on each dataset is highlighted in **boldface** under different cases of supervision. ‘Sup.’ denotes for supervision information. ‘F’ means fully supervised. ‘I’ means image-level supervised. ‘S’ means scribble-level supervised. ‘M’ means multi-source supervised and ‘Un’ is for unsupervised. ‘ \dagger ’ means two-round training.

Methods	Sup.	ECSSD			DUT-OMRON			PASCAL-S		
		$F_\beta \uparrow$	$E_\xi \uparrow$	$MAE \downarrow$	$F_\beta \uparrow$	$E_\xi \uparrow$	$MAE \downarrow$	$F_\beta \uparrow$	$E_\xi \uparrow$	$MAE \downarrow$
DGRL (2018)	F	0.9027	0.9371	0.043	0.7264	0.8446	0.0632	0.8289	0.8353	0.1150
PiCANet (2018)	F	0.8864	0.9128	0.0464	0.7173	0.8407	0.0653	0.7979	0.8330	0.0750
PAGR(2018b)	F	0.8718	0.8869	0.0644	0.6754	0.7717	0.0709	0.7656	0.7545	0.1516
MLMSNet (2019)	F	0.8856	0.9218	0.0479	0.7095	0.8306	0.0636	0.8129	0.8219	0.1193
CPD (2019)	F	0.917	0.925	0.037	0.747	0.866	0.056	0.824	0.849	0.072
AFNet (2019)	F	0.9008	0.9294	0.0450	0.7425	0.8456	0.0574	0.8241	0.8269	0.1155
PFAN (2019)	F	0.8592	0.8636	0.0467	0.7009	0.7990	0.0615	0.7544	0.7464	0.1372
BASNet (2019)	F	0.880	0.916	0.037	0.756	0.869	0.056	0.775	0.832	0.076
GCPANet (2020)	F	0.9184	0.927	0.035	0.7479	0.839	0.056	0.8335	0.861	0.061
MINet (2020)	F	0.924	0.953	0.033	0.756	0.873	0.055	0.842	0.899	0.064
SVF (2017)	Un	0.7823	0.8354	0.0955	0.6120	0.7633	0.1076	0.7351	0.7459	0.1669
MNL (2018a)	Un	0.8098	0.8357	0.0902	0.5966	0.7124	0.1028	0.7476	0.7408	0.1576
ASMO (2018)	I	0.7621	0.7921	0.0681	0.6408	0.7605	0.0999	0.6532	0.6474	0.2055
WSS (2017)	I	0.7672	0.7693	0.1081	0.5895	0.7292	0.1102	0.6975	0.6904	0.1843
MSW (2019)	M	0.7606	0.7876	0.0980	0.5970	0.7283	0.1087	0.6850	0.6932	0.1780
WSSA (2020b)	S	0.845	0.898	0.068	0.679	0.823	0.074	0.772	0.791	0.145
WSSA \dagger (2020b)	S	0.8650	0.9077	0.0610	0.7015	0.8345	0.0684	0.7884	0.7975	0.1399
Ours	S	0.8995	0.9079	0.0489	0.7580	0.8624	0.0602	0.8230	0.8465	0.0779
Methods	Sup.	HKU-IS			THUR			DUTS-TEST		
		$F_\beta \uparrow$	$E_\xi \uparrow$	$MAE \downarrow$	$F_\beta \uparrow$	$E_\xi \uparrow$	$MAE \downarrow$	$F_\beta \uparrow$	$E_\xi \uparrow$	$MAE \downarrow$
DGRL (2018)	F	0.8844	0.9388	0.0374	0.7271	0.8378	0.0774	0.7989	0.8873	0.0512
PiCANet (2018)	F	0.8704	0.9355	0.0433	-	-	-	0.7589	0.8616	0.0506
PAGR(2018b)	F	0.8638	0.8979	0.0475	0.7395	0.8417	0.0704	0.7781	0.8422	0.0555
MLMSNet (2019)	F	0.8780	0.9304	0.0387	0.7177	0.8288	0.0794	0.7917	0.8829	0.0490
CPD (2019)	F	0.891	0.944	0.034	-	-	-	0.805	0.886	0.043
AFNet (2019)	F	0.8877	0.9344	0.0358	0.7327	0.8398	0.0724	0.8123	0.8928	0.0457
PFAN (2019)	F	0.8717	0.8982	0.0424	0.6833	0.8038	0.0939	0.7648	0.8301	0.0609
BASNet (2019)	F	0.895	0.946	0.032	0.7366	0.8408	0.0734	0.791	0.884	0.048
GCPANet (2020)	F	0.8984	0.920	0.031	-	-	-	0.8170	0.891	0.038
MINet (2020)	F	0.908	0.961	0.028	-	-	-	0.828	0.917	0.037
SVF (2017)	Un	0.7825	0.8549	0.0753	0.6269	0.7699	0.1071	0.6223	0.7629	0.1069
MNL (2018a)	Un	0.8196	0.8579	0.0650	0.6911	0.8073	0.0860	0.7249	0.8525	0.0749
ASMO (2018)	I	0.7625	0.7995	0.0885	-	-	-	0.5687	0.6900	0.1156
WSS (2017)	I	0.7734	0.8185	0.0787	0.6526	0.7747	0.0966	0.6330	0.8061	0.1000
MSW (2019)	M	0.7337	0.7862	0.0843	-	-	-	0.6479	0.7419	0.0912
WSSA (2020b)	S	0.835	0.911	0.055	0.696	0.824	0.085	0.728	0.857	0.068
WSSA \dagger (2020b)	S	0.8576	0.9232	0.0470	0.7181	0.8367	0.0772	0.7467	0.8649	0.0622
Ours	S	0.8962	0.9376	0.0375	0.7545	0.8430	0.0693	0.8226	0.8904	0.0487

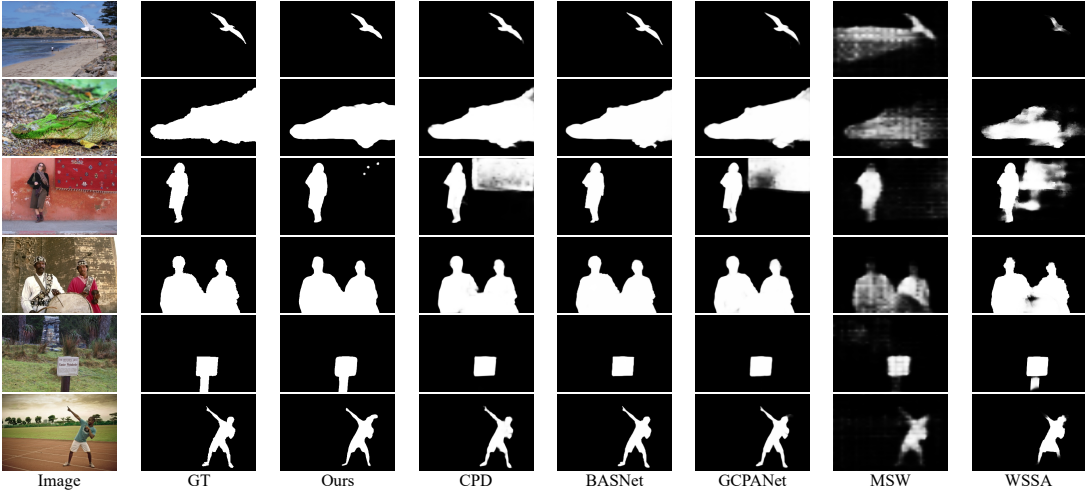


Figure 5: Qualitative comparisons of saliency maps predicted by our method and other state-of-the-art methods. Obviously, the maps predicted by ours are closer to the ground-truth compared with other weakly supervised approaches (MSW (Zeng et al. 2019) & WSSA (Zhang et al. 2020b)), and some of our results even cover more details than that of fully supervised approaches (CPD (Wu, Su, and Huang 2019), BASNet (Qin et al. 2019), GCPANet (Chen et al. 2020)) as in row 5.

Table 2: Ablation study for our losses and AGGM on DUTS-TEST dataset. ‘Base.’ denotes for baseline and ‘A.’ denotes for AGGM. Our overall method obtains the best results.

	Base.	A.	\mathcal{L}_{ssc}	\mathcal{L}_{lsc}	$F_\beta \uparrow$	$E_\xi \uparrow$	$MAE \downarrow$
1	✓				0.707	0.843	0.064
2	✓		✓		0.706	0.845	0.064
3	✓		✓	✓	0.758	0.873	0.059
4	✓	✓	✓	✓	0.823	0.890	0.049

Table 3: Ablation study for our proposed AGGM on DUT-OMRON and DUTS-TEST datasets. It can be seen that our AGGM is compatible to our loss functions.

	DUT-OMRON			DUTS-TEST		
	$F_\beta \uparrow$	$E_\xi \uparrow$	$MAE \downarrow$	$F_\beta \uparrow$	$E_\xi \uparrow$	$MAE \downarrow$
w/o	0.730	0.845	0.069	0.800	0.877	0.053
w/	0.758	0.862	0.060	0.823	0.890	0.049

Table 4: Ablation study for SSIM in the saliency structure consistency loss on DUT-OMRON and DUTS-TEST.

	DUT-OMRON			DUTS-TEST		
	$F_\beta \uparrow$	$E_\xi \uparrow$	$MAE \downarrow$	$F_\beta \uparrow$	$E_\xi \uparrow$	$MAE \downarrow$
w/o	0.670	0.828	0.077	0.735	0.863	0.063
w/	0.708	0.841	0.072	0.758	0.873	0.059

the scores of the three evaluation metrics with SSIM are all higher than those without SSIM, which indicates that Eq. (6) needs SSIM to make better prediction.

Impact of Local Saliency Coherence Loss. We list the evaluation of the local saliency coherence loss in Table 2. With our local saliency coherence loss, the network can obtain the best results. Specifically, using local saliency coherence loss improves F_β from 0.7584 to 0.8226, E_ξ from 0.8732 to 0.8904 and MAE from 0.0589 to 0.0487. It is the new state-of-the-art performance as reported in Table 1. Since there is no extra supervision information like edges, such performance demonstrates that our local saliency coherence loss can learn integral salient object structures.

Conclusions

In this paper, we have explored one-round training for salient object detection via scribble annotations. We propose a local saliency coherence loss to supervise unlabeled points. Besides, we deploy a self-consistent mechanism via saliency structure consistency loss to improve the network generalization ability. Moreover, we have designed an aggregation module to better integrate multiple levels of features, so as to predict better saliency maps for weakly supervised SOD. Experiments show that our approach outperforms previous state-of-the-arts under different evaluation metrics on 6 datasets with a significant margin. Furthermore, our proposed loss functions utilize intrinsic properties of input images to supervise unlabeled points, such that no extra supervision is introduced.

Acknowledgment

The work was supported by National Natural Science Foundation of China under 61972323, and Key Program Special Fund in XJTLU under KSF-T-02, KSF-P-02.

References

- Bearman, A.; Russakovsky, O.; Ferrari, V.; and Fei-Fei, L. 2016. What’s the point: Semantic segmentation with point supervision. In *European conference on computer vision (ECCV)*.
- Chen, D.-J.; Chien, J.-T.; Chen, H.-T.; and Chang, L.-W. 2018. Tap and shoot segmentation. In *Proceedings of the Thirty-second AAAI Conference on Artificial Intelligence (AAAI)*.
- Chen, Z.; Xu, Q.; Cong, R.; and Huang, Q. 2020. Global Context-aware Progressive Aggregation Network for Salient Object Detection. In *Proceedings of the Thirty-fourth AAAI Conference on Artificial Intelligence (AAAI)*.
- Cheng, M.-M.; Mitra, N. J.; Huang, X.; and Hu, S.-M. 2014. Salientshape: Group Saliency in Image Collections. *The Visual Computer* 30(4): 443–453.
- Cong, R.; Lei, J.; Fu, H.; Lin, W.; Huang, Q.; Cao, X.; and Hou, C. 2017. An Iterative Co-saliency Framework for RGBD Images. *IEEE Transactions on Cybernetics* 49(1): 233–246.
- Deng, J.; Dong, W.; Socher, R.; Li, L.-J.; Li, K.; and Fei-Fei, L. 2009. Imagenet: A large-scale Hierarchical Image Database. In *Proceedings of the IEEE/CVF Conference on Computer Vision and Pattern Recognition (CVPR)*.
- Fan, D.-P.; Gong, C.; Cao, Y.; Ren, B.; Cheng, M.-M.; and Borji, A. 2018. Enhanced-alignment Measure for Binary Foreground Map Evaluation.
- Feng, M.; Lu, H.; and Ding, E. 2019. Attentive Feedback Network for Boundary-aware Salient Object Detection. In *Proceedings of the IEEE/CVF Conference on Computer Vision and Pattern Recognition (CVPR)*.
- Godard, C.; Mac Aodha, O.; and Brostow, G. J. 2017. Unsupervised Monocular Depth Estimation with Left-right Consistency. In *Proceedings of the IEEE/CVF Conference on Computer Vision and Pattern Recognition (CVPR)*.
- He, K.; Zhang, X.; Ren, S.; and Sun, J. 2016. Deep Residual Learning for Image Recognition. In *Proceedings of the IEEE/CVF Conference on Computer Vision and Pattern Recognition (CVPR)*.
- Hou, Q.; Cheng, M.-M.; Hu, X.; Borji, A.; Tu, Z.; and Torr, P. H. 2017. Deeply Supervised Salient Object Detection with Short Connections. In *Proceedings of the IEEE/CVF Conference on Computer Vision and Pattern Recognition (CVPR)*.
- Ji, Z.; Wang, H.; Han, J.; and Pang, Y. 2019. Saliency-Guided Attention Network for Image-Sentence Matching. In *Proceedings of the IEEE/CVF International Conference on Computer Vision (ICCV)*.
- Khoreva, A.; Benenson, R.; Hosang, J.; Hein, M.; and Schiele, B. 2017. Simple does it: Weakly supervised instance and semantic segmentation. In *Proceedings of the IEEE/CVF Conference on Computer Vision and Pattern Recognition (CVPR)*.
- Li, G.; Xie, Y.; and Lin, L. 2018. Weakly Supervised Salient Object Detection Using Image Labels. In *Proceedings of the Thirty-second AAAI Conference on Artificial Intelligence (AAAI)*.
- Li, G.; and Yu, Y. 2015. Visual Saliency based on Multiscale Deep Features. In *Proceedings of the IEEE/CVF Conference on Computer Vision and Pattern Recognition (CVPR)*.
- Li, Y.; Hou, X.; Koch, C.; Rehg, J. M.; and Yuille, A. L. 2014. The Secrets of Salient Object Segmentation. In *Proceedings of the IEEE/CVF Conference on Computer Vision and Pattern Recognition (CVPR)*.
- Lin, D.; Dai, J.; Jia, J.; He, K.; and Sun, J. 2016. Scribble-Sup: Scribble-Supervised Convolutional Networks for Semantic Segmentation. In *Proceedings of the IEEE/CVF Conference on Computer Vision and Pattern Recognition (CVPR)*.
- Liu, J.-J.; Hou, Q.; Cheng, M.-M.; Feng, J.; and Jiang, J. 2019. A Simple Pooling-Based Design for Real-Time Salient Object Detection. In *Proceedings of the IEEE/CVF Conference on Computer Vision and Pattern Recognition (CVPR)*.
- Liu, N.; Han, J.; and Yang, M.-H. 2018. Picanet: Learning Pixel-wise Contextual Attention for Saliency Detection. In *Proceedings of the IEEE/CVF Conference on Computer Vision and Pattern Recognition (CVPR)*.
- Maninis, K.-K.; Caelles, S.; Pont-Tuset, J.; and Van Gool, L. 2018. Deep Extreme Cut: From Extreme Points to Object Segmentation. In *Proceedings of the IEEE/CVF Conference on Computer Vision and Pattern Recognition (CVPR)*.
- Nguyen, T.; Dax, M.; Mummadgi, C. K.; Ngo, N.; Nguyen, T. H. P.; Lou, Z.; and Brox, T. 2019. DeepUSPS: Deep Robust Unsupervised Saliency Prediction via Self-supervision. In *Proceedings of the Advances in Neural Information Processing Systems 32*.
- Obukhov, A.; Georgoulis, S.; Dai, D.; and Van Gool, L. 2019. Gated CRF Loss for Weakly Supervised Semantic Image Segmentation. *arXiv preprint arXiv:1906.04651* .
- Pang, Y.; Zhao, X.; Zhang, L.; and Lu, H. 2020. Multi-Scale Interactive Network for Salient Object Detection. In *Proceedings of the IEEE/CVF Conference on Computer Vision and Pattern Recognition (CVPR)*.
- Qin, X.; Zhang, Z.; Huang, C.; Gao, C.; Dehghan, M.; and Jagersand, M. 2019. BASNet: Boundary-Aware Salient Object Detection. In *Proceedings of the IEEE/CVF Conference on Computer Vision and Pattern Recognition (CVPR)*.
- Shi, B.; Dai, Q.; Mu, Y.; and Wang, J. 2020. Weakly-Supervised Action Localization by Generative Attention Modeling. In *Proceedings of the IEEE/CVF Conference on Computer Vision and Pattern Recognition (CVPR)*.
- Song, C.; Huang, Y.; Ouyang, W.; and Wang, L. 2019. Box-Driven Class-Wise Region Masking and Filling Rate Guided Loss for Weakly Supervised Semantic Segmentation. In *Proceedings of the IEEE/CVF Conference on Computer Vision and Pattern Recognition (CVPR)*.

- Sun, F.; and Li, W. 2019. Saliency Guided Deep Network for Weakly-Supervised Image Segmentation. *Pattern Recognition Letters* 120: 62–68.
- Tang, M.; Djelouah, A.; Perazzi, F.; Boykov, Y.; and Schroers, C. 2018a. Normalized Cut Loss for Weakly-Supervised CNN Segmentation. In *Proceedings of the IEEE Conference on Computer Vision and Pattern Recognition (CVPR)*.
- Tang, M.; Perazzi, F.; Djelouah, A.; Ben Ayed, I.; Schroers, C.; and Boykov, Y. 2018b. On Regularized Losses for Weakly-supervised CNN Segmentation. In *Proceedings of the IEEE/CVF Conference on European Conference on Computer Vision (ECCV)*.
- Wang, H.; Li, Z.; Li, Y.; Gupta, B.; and Choi, C. 2020a. Visual Saliency Guided Complex Image Retrieval. *Pattern Recognition Letters* 130: 64–72.
- Wang, L.; Lu, H.; Wang, Y.; Feng, M.; Wang, D.; Yin, B.; and Ruan, X. 2017. Learning to Detect Salient Objects with Image-level Supervision. In *Proceedings of the IEEE/CVF Conference on Computer Vision and Pattern Recognition (CVPR)*.
- Wang, T.; Zhang, L.; Wang, S.; Lu, H.; Yang, G.; Ruan, X.; and Borji, A. 2018. Detect Globally, Refine Locally: A Novel Approach to Saliency Detection. In *Proceedings of the IEEE/CVF Conference on Computer Vision and Pattern Recognition (CVPR)*.
- Wang, W.; Zhao, S.; Shen, J.; Hoi, S. C. H.; and Borji, A. 2019. Salient Object Detection With Pyramid Attention and Salient Edges. In *Proceedings of the IEEE/CVF Conference on Computer Vision and Pattern Recognition (CVPR)*.
- Wang, Y.; Zhang, J.; Kan, M.; Shan, S.; and Chen, X. 2020b. Self-supervised Equivariant Attention Mechanism for Weakly Supervised Semantic Segmentation. In *Proceedings of the IEEE/CVF Conference on Computer Vision and Pattern Recognition (CVPR)*.
- Wang, Z.; Bovik, A. C.; Sheikh, H. R.; and Simoncelli, E. P. 2004. Image Quality Assessment: from Error Visibility to Structural Similarity. *IEEE Transactions on Image Processing* 13(4): 600–612.
- Wu, R.; Feng, M.; Guan, W.; Wang, D.; Lu, H.; and Ding, E. 2019. A Mutual Learning Method for Salient Object Detection with Intertwined Multi-supervision. In *Prceedings of the IEEE/CVF Conference on Computer Vision and Pattern Recognition (CVPR)*.
- Wu, Z.; Su, L.; and Huang, Q. 2019. Cascaded Partial Decoder for Fast and Accurate Salient Object Detection. In *Proceedings of the IEEE/CVF Conference on Computer Vision and Pattern Recognition (CVPR)*.
- Yan, Q.; Xu, L.; Shi, J.; and Jia, J. 2013. Hierarchical Saliency Detection. In *Proceedings of the IEEE/CVF Conference on Computer Vision and Pattern Recognition (CVPR)*.
- Yang, C.; Zhang, L.; Lu, H.; Ruan, X.; and Yang, M.-H. 2013. Saliency Detection via Graph-based Manifold Rank-
ing. In *Proceedings of the IEEE/CVF Conference on Computer Vision and Pattern Recognition (CVPR)*.
- Zeng, Y.; Zhuge, Y.; Lu, H.; Zhang, L.; Qian, M.; and Yu, Y. 2019. Multi-source Weak Supervision for Saliency Detection. In *Proceedings of the IEEE/CVF Conference on Computer Vision and Pattern Recognition (CVPR)*.
- Zhang, B.; Xiao, J.; Wei, Y.; Sun, M.; and Huang, K. 2020a. Reliability Does Matter: An End-to-End Weakly Supervised Semantic Segmentation Approach. In *Proceedings of the Thirty-fourth AAAI Conference on Artificial Intelligence (AAAI)*.
- Zhang, D.; Han, J.; and Zhang, Y. 2017. Supervision by Fusion: Towards Unsupervised Learning of Deep Salient Object Detector. In *Proceedings of the IEEE/CVF International Conference on Computer Vision (ICCV)*.
- Zhang, J.; Yu, X.; Li, A.; Song, P.; Liu, B.; and Dai, Y. 2020b. Weakly-Supervised Salient Object Detection via Scribble Annotations. In *Proceedings of the IEEE/CVF Conference on Computer Vision and Pattern Recognition (CVPR)*.
- Zhang, J.; Zhang, T.; Dai, Y.; Harandi, M.; and Hartley, R. 2018a. Deep Unsupervised Saliency Detection: A Multiple Noisy Labeling Perspective. In *Proceedings of the IEEE/CVF Conference on Computer Vision and Pattern Recognition (CVPR)*.
- Zhang, X.; Wang, T.; Qi, J.; Lu, H.; and Wang, G. 2018b. Progressive Attention Guided Recurrent Network for Salient Object Detection. In *Proceedings of the IEEE/CVF Conference on Computer Vision and Pattern Recognition (CVPR)*.
- Zhao, J.-X.; Liu, J.-J.; Fan, D.-P.; Cao, Y.; Yang, J.; and Cheng, M.-M. 2019. EGNet: Edge Guidance Network for Salient Object Detection. In *Proceedings of the IEEE/CVF International Conference on Computer Vision (ICCV)*.
- Zhao, T.; and Wu, X. 2019. Pyramid Feature Attention Network for Saliency Detection. In *Proceedings of the IEEE/CVF Conference on Computer Vision and Pattern Recognition (CVPR)*.